Paper Number 01ICES-2326

Deep Space Mission Radiation Shielding Optimization

R. K. Tripathi, J. W. Wilson
NASA Langley Research Center, Hampton, VA

F. A. Cucinotta
NASA Johnson Space Center, Houston, TX

J. E. Nealy
Old Dominion University, Norfolk, VA

M. S. Clowdsley
National Research Council/NASA Langley Research Center, Hampton, VA

M.-H. Y. Kim
College of William and Mary, Williamsburg, VA

ABSTRACT

Providing protection against the hazards of space radiation is a major challenge to the exploration and development of space. The great cost of added radiation shielding is a potential limiting factor in deep space missions. In the present report, we present methods for optimized shield design over multi-segmented missions involving multiple work and living areas in the transport and duty phase of lunar and Mars missions. The total shield mass over all pieces of equipment and habitats is optimized subject to career dose and dose rate constraints.

INTRODUCTION

An enabling technology for the exploration, the development, and the commercialization of space is a cost-effective means of reducing the health risks from exposures to galactic cosmic rays (GCR) and a possible solar particle event (SPE). This has been a well-recognized challenge and a critical enabling technology for exploration in which astronaut health effects are of principal concern. Even more so with the development of space infrastructure and the eventual commercialization of space as new materials and other space products are identified and as larger numbers of civilians become involved in space based careers. At the present stage of space exploration, the astronaut corps is a select group of individuals who normally enter into service near mid-life and have a very limited career duration that allows unusually high annual exposures during their short career. Even then the mitigation of health risks is a great challenge. As we begin to build infrastructure for commercialization, the involvement of more ordinary career workers who will live and work in space will require a reassessment of allowable exposure limits and undoubtedly a substantial reduction in allowable annual exposure. Even more challenging is the "personal family explorer" who may choose to have a family vacation in space. The use of shielding to control exposure and the role of pharmacology in risk mitigation are critical issues in space development.

Shield mass can be a high cost factor in system designs for the long-term operations required and optimization methods in the design process will be critical to cost-effective progress in space development [1]. Limiting the time of transfer to duty station or the mission time within the solar cycle as well as the choice of materials used in construction can reduce the shield mass required on specific missions [2]. Unfortunately, adequate optimization procedures have not been available to minimize the mass and the associated costs for a given mission scenario.

Much of the protection within a space structure is provided by the structural elements, onboard materials, and equipment required for other purposes and the means of making the best choice of materials among various options is critical to the protective qualities of the overall design. Multifunctionality of materials (for example, structural elements which have good shielding properties) will be common in the optimization process. Furthermore, the design decisions cannot be made in a vacuum and multidisciplinary design methods need to be

developed. The need for multifunctional/multidisciplinary design techniques was identified as critical to the cost-effective development of space several years ago [1] and expanded on recently [2].

In the past an amount of exposure was assigned to each mission segment and developed as a subjective strategy with relative improvements of costs through material trades dependent on off-optimum design solutions. It is the purpose of the present study to develop the necessary optimization methods for minimum mass determinations to be used in performing trade studies to enable objective trade reduction costs since strategies for meeting exposure constraints are optimized over the entire mission architecture for each trade. In addition to optimized design trades, we will also consider the implementation of the principle of as low as reasonably achievable (ALARA) required by federal regulation and normally ignored in mission design studies. The ALARA principle will be met by added protection of the crew quarters where members will spend a significant fraction of each day sleeping. The main crew quarter design will also be used as the shelter from potential solar particle events during the mission. In this respect, we assume an adequate strategy for exposure limitation during EVA activity is available and the design is mainly the habitable volume and crew quarter/SPE shelter. Emergency planning in the case of an accidental SPE exposure will have to be part of the overall mission plan and is not considered in the present study.

In the present study, we will consider an 860 day Mars Reference Mission, a baseline 47 day Lunar mission, and a baseline 62 day L2 mission to a deep space platform assuming Al 2219 as the reference construction material. Trades on materials for construc-tion of the living/working space and crew quarter shielding and impact on costs through a change in launch mass will be used to quantify the savings. In addition to the material trade studies, propulsion engine trade studies can be performed by change in mission scenario time lines.

EXPOSURE AND OTHER CONSTRAINTS

The present exposure constraints used in the space program are recommended for low Earth orbit (LEO) operations by the National Council on Radiation Protection [3] and approved by the NASA Administrator and OSHA. There are no limits for deep space operations due to the unusual composition of the GCR and the resultant uncertainties in associated health risks. The NCRP did recommend that the limits for low earth orbit (LEO) operations could be used as a guide in deep space operational studies [3]. New exposure recom-mendations are now approved by the NCRP [4] and the new LEO limits are given the three critical organs of skin, ocular lens, and blood forming organ (BFO) in tables 1 and 2 and will be used herein recognizing the associated uncertainties. We use dose equivalent for the Gy-Eq since insufficient data will not allow Gy-Eq evaluation at this time.

In the present work, the optimized mission will be taken as the minimum mass to meet mission requirements and not exceed the exposure constraints in tables 1 and 2. The present design considerations are for the main habitable areas. The volume limited crew quarters where a large fraction of personal time is spent will have added protection to further reduce exposures (ALARA) and will also be designed to provide the shelter from a solar particle event.

Table 1—Recommended organ dose equivalent limits for all ages.

	BFO, Sv	Eye, Sv	Skin, Sv
Career	See Table 2	4.0	6.0
Annual	0.50	2.0	3.0
30 Days	0.25	1.0	1.5

Table 2—Career whole body-dose equivalent limit (Sv) for lifetime excess risk of fatal cancer of three percent as a function of age at exposure.

Age	25	35	45	55
Male	0.7	1.0	1.5	2.9
Female	0.4	0.6	0.9	1.6

Aside from the radiation health risks, the psychological well being and its impact on crew performance also affects the shield design [5]. Crew performance level is related in part to the length of the mission and the volume of the work/living areas of the spacecraft. The design performance levels of Optimal, Performance Limit, and Tolerable are shown in figure 1 as a function of duration of the stay. Rather small volumes are useful over short time periods but long missions require sufficient space for a crew to perform at reasonable levels. We will use the Optimal design for the habitable volume and the Tolerable design for the crew quarters which will also serve as the SPE shelter.

Table 3 -- Performance levels descriptions

Performance index	Performance level description
1	Optimal performance limit best suited for long duration with minimal impact on crew performance
2	Performance limit allows crew demands to be met but not well suited for long duration
3	Tolerable limit provides space for astronaut to survive but not well suited for other than emergencies

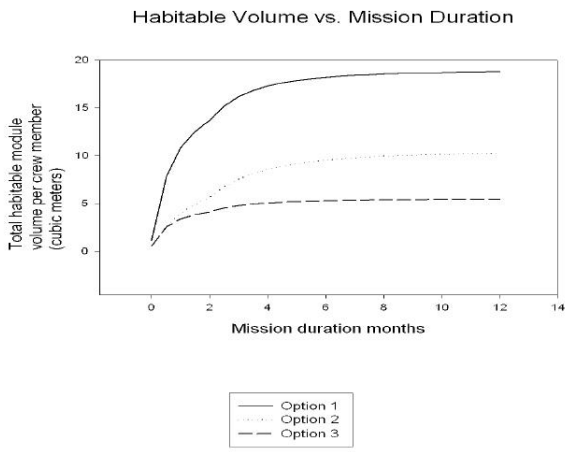

Fig. 1. Habitable volume for given mission duration.

SPACE ENVIRONMENT AND SHIELDING MATERIALS

In order to quantify radiation exposure in space, it is required that the external ambient ionizing radiation environment be specified in terms of individual constituents and their respective energy fluxes. A great quantity of observational space environmental data from instrumented space platforms has been amassed in recent decades and used in developing computer models serving to define, as well as possible, the composition and temporal behavior of the space environment [6]. From the standpoint of radiation protection for humans in interplanetary space, the heavy ions (atomic nuclei with all electrons removed) of the galactic cosmic rays (GCR) and the sporadic production of energetic protons from large solar particle events (SPE) must be dealt with. The GCR environmental model used herein is based on a current version in which ion spectra are modulated between solar maxima and minima according to terrestrial neutron monitor data assuming the radial dependent diffusion model of Badhwar et al. [7], as described in reference [8] by Wilson et al. The modeled spectra for Solar minimum in 1977 and Solar Maximum in 1990 as given by Badhwar are shown in figure 2. The required historic and projected Sunspot numbers along with the corresponding Deep River Neutron Monitor count rates are shown in figure 3. There is only a few percent difference between the environment measured near Earth and what is observed near Mars and other locations near the Earth's orbit about the sun. These anticipated differences are less than the model uncertainty and will be ignored in the present study.

The environment near a large celestial body is modified by interaction with local materials producing an induced environment and shielding within the subtended angle of such a large body. The surface exposure on a lunar plain is shielded below the horizon but experiences an induced environment (mainly but not exclusively neutrons) produced in the local surface. The lunar surface GCR environment is shown in figure 4 at the 1977 Solar Minimum and the 1990 Solar Maximum. In addition to the GCR ions streaming from overhead, large numbers of neutrons are produced in the lunar surface materials and diffuse from below the surface as shown in the figure. Similar results are shown on the surface of Mars in figure 5. The main difference is the presence of the Martian atmosphere that attenuates the incident ions and produces additional GCR fragments and more energetic neutrons produced in the atmosphere overhead.

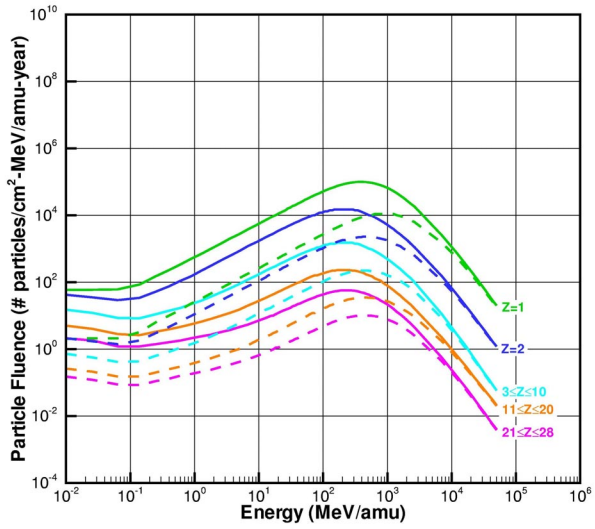

Fig. 2. Galactic cosmic ray spectra at the 1997 Solar Minimum (full lines) and 1990 Solar Maximum (dashed lines) according to Badhwar et al.

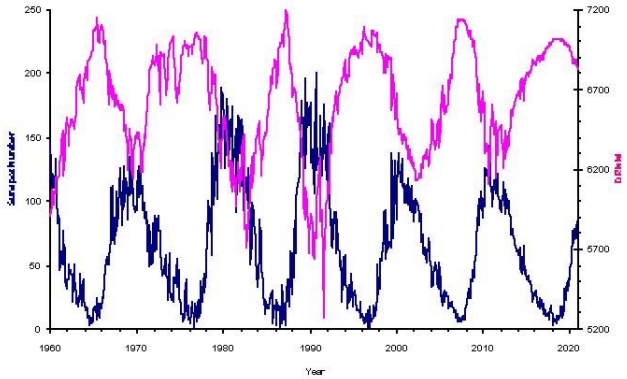

Fig. 3. Sunspot number (blue) and Deep River Neutron Monitor (pink) count rate for 1960 to 2022.

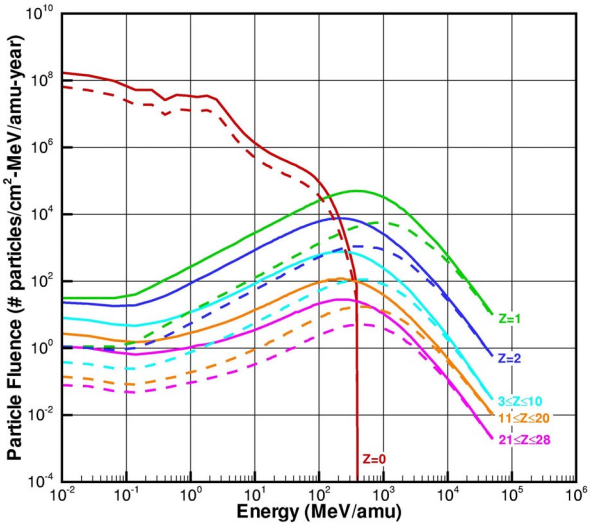

Fig. 4. GCR environment during the 1977 Solar Minimum (full lines) and the 1990 Solar Maximum (dashed lines) on the lunar surface.

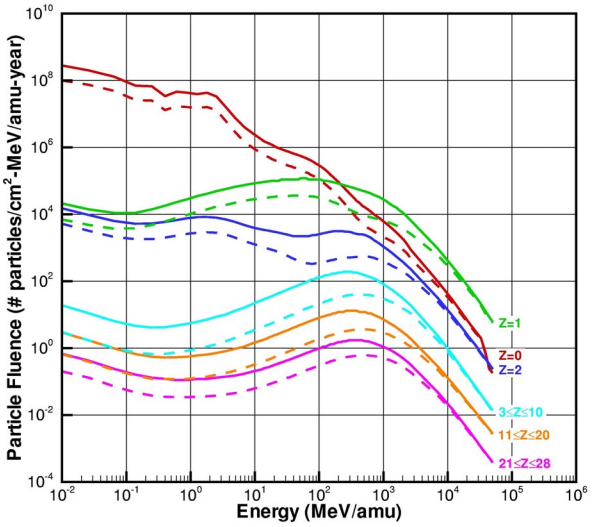

Fig. 5. GCR environment during the 1977 Solar minimum and the 1990 Solar Maximum on the Martian surface (mean altitude) using the Marsgram atmospheric model.

Large SPE have only been observed to occur during times of increased solar activity conditions, and very large energetic events of grave important to human protection occur only infrequently (avg. 1 or 2 per cycle) and only outside of two years of solar minimum. Among the large events, the largest observed ground level event of the last 60 years of observation is that of February 23, 1956 which produced a 3600 percent increase in neutron monitor levels on the terrestrial surface. The next largest event observed is the September 29, 1989 event with ground level increases of 400 percent or an order of magnitude smaller than that of Feb. 1956 event. Numerous other ground level events of smaller magnitude have occurred but are a factor of four and more lower in magnitude than the Sept. 1989 event. It is known that large SPEs are potentially mission threatening, and astronauts in deep space must have access to adequate shelter from such an occurrence. The SPE particle energy spectrum used here has been derived from the event which took place on September 29, 1989. To provide a baseline worst-case scenario we assume an event of the order of four times larger than the September 29, 1989 event as an event comparable to the August 4, 1972 event from the point of view of space exposure. The September 1989 SPE spectrum is shown in figure 6. If we meet 30-day dose rate constraints on an event four times larger than the September 1989 event then it is unlikely that an added factor of two or so larger events (like that of Feb. 23, 1956) would have serious medical consequences. The rationale and plausibility for this model is described by Kim et al. [9].

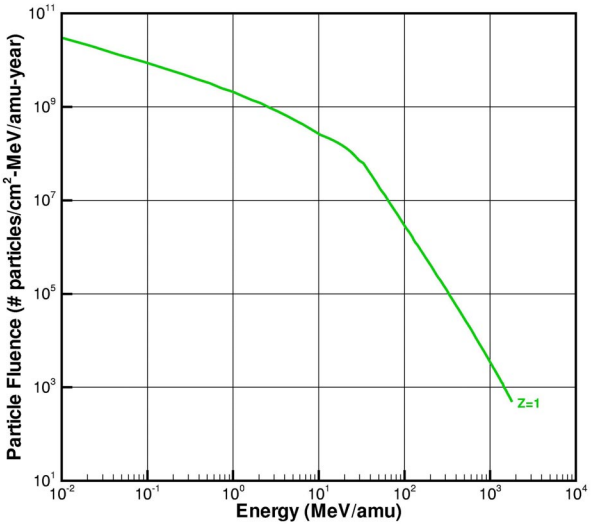

Fig. 6. SPE spectrum during September 1989 as observed near Earth.

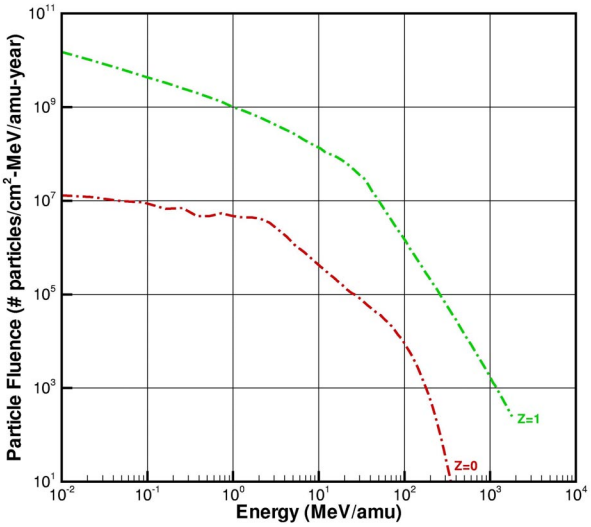

Fig. 7. The lunar surface environment during the September 1989 SPE.

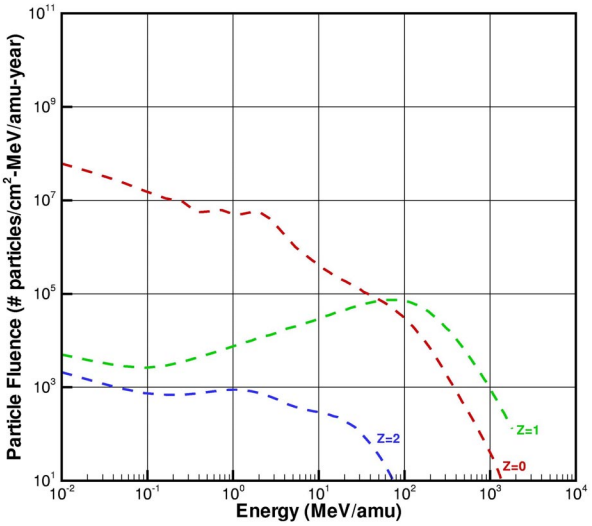

Fig. 8. The Martian surface environment during the September 1989 SPE.

The SPE are likewise altered by the presence of a large body similar to the GCR. The corresponding lunar surface and Martian surface environments are shown in figures 7 and 8. The role of the neutrons on the lunar surface is less effective in causing exposure relative to the protons streaming from overhead. Note that is in contrast to the more energetic GCR wherein large numbers of neutrons are produced in the lunar surface materials (see figure 7). Neutrons play a relatively more important role on the Martian surface where added neutrons are produced in the overhead atmosphere and the SPE protons are greatly attenuated.

The effectiveness of a given shield material is characterized by the transport of energetic particles within the shield, which is in turn defined by the interactions of the local environmental particles (and in most cases, their secondaries) with the constituent atoms and nuclei of the shield material. These interactions vary greatly with different material types. Materials in the present study are given in table 4. For space radiation shields, materials with high hydrogen content generally have greater shielding effectiveness, but often do not possess qualities that lend themselves to the required structural integrity of the space vehicle or habitat. Organic polymers are the exception. The design of properly-shielded spacecraft and habitats for long-duration human presence in interplanetary space will thus require an approach tending toward optimization of a compromise between protective shielding and various other functional aspects of the onboard materials. Candidate multifunctional materials for such an optimization approach have been chosen here to represent various contributing elements in a vehicle shield design. Liquid hydrogen and methane are possible fuels that in large quantities may contribute substantially to overall protection. Aluminum has long been a spacecraft material of choice although various forms of polymeric materials show enhanced protection properties such as polyethylene. The polysulfone and polyetherimide are high performance structural polymers. Lithium hydride is a popular shield material for nuclear power reactors, but is generally not useful for other functions. The graphite nanofiber materials heavily impregnated with hydrogen may well represent a viable multifunctional component in future space structures, and its inclusion here should presently be considered as not yet state-of-the-art.

Table 4. Chemical composition of materials used in the present study

Material	ID	Atom	Z	A	atoms/g	Density g/cm²
Aluminum 2219	ALM	Al	13	27	2.08E+22	2.83
		Ti	22	48	7.53E+18	
		V	23	51	1.18E+19	
		Mn	25	55	3.31E+19	
		Cu	29	64	5.90E+20	
		Zr	40	91	1.19E+19	
Poly-etherimide	PEI	H	1	1	2.44E+22	1.27
		C	6	12	3.76E+22	
		N	7	14	2.03E+21	
		O	8	16	6.10E+21	
Polysulfone	PSF	H	1	1	3.00E+22	1.24
		C	6	12	3.68E+22	
		O	8	16	5.45E+21	
		S	16	32	1.36E+21	
Poly-ethylene	PET	H	1	1	8.60E+22	0.92
		C	6	12	4.30E+22	
Lithium Hydride	LIH	H	1	1	7.53E+22	0.82
		Li	3	7	7.53E+22	
Liquid Methane	LME	H	1	1	1.51E+23	0.466
		C	6	12	3.76E+22	
Graphite Nanofibers	GNF	H	1	1	4.07E+23	2.25
		C	6	12	1.63E+22	
Liquid Hydrogen	LH2	H	1	1	6.03E+23	0.07

The results of detailed transport calculations for these materials have been incorporated into a shield design database. Important in this respect is their chemical composition and mass density given in table 4. The shield effectiveness for the above-discussed environments were evaluated using the HZETRN code with improved neutron transport procedures [10]. The exposures to critical organ tissues were evaluated for each environment within spherical shells of each material. The time dependent dose rates are evaluated within the shielding materials assuming exposure in the center of a large volume with varying wall thickness. The annual dose rates within the Al 2219 alloy shield are shown for ocular lens and BFO in figures 9 and 10. Large variations in exposure of critical organs are seen to occur over time and with increasing shielding.

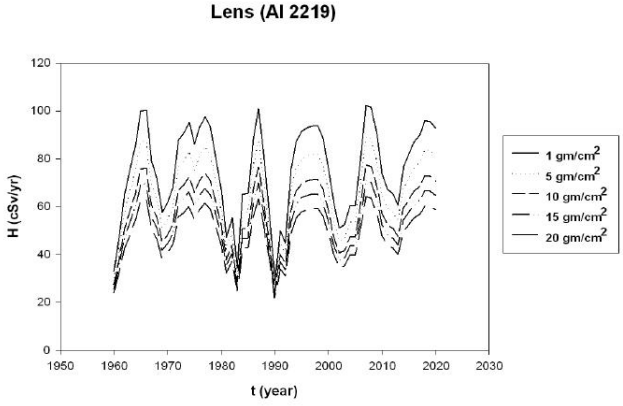

Fig. 9. Annual dose equivalent to ocular lens within an Al 2219 shielded region.

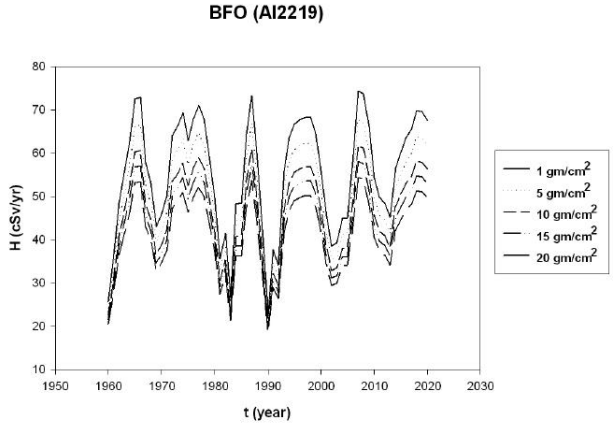

Fig. 10. Annual dose equivalent to BFO within an Al 2219 shielded region.

CONSTRAINTS AND OPTIMIZATION

The general principles required to optimize a mission is implemented in this section. In the absence of a specific design, we start with assumptions to be used in estimating exposures and shield mass. A baseline vehicle design will include Al 2219 alloy construction and evaluate shield mass assuming 40% of the solid angle is shielded by vehicle components constructed of Al alloy (assumed to be 30 g/cm^2 over 15% of the solid angle and 60 g/cm^2 for the remaining 25%) and normally different than the shield material comprising the remaining 60% of the total solid angle. Only the shield mass requirements for the remaining 60% of the solid angle is taken herein as shielding. Lacking a specific vehicle design, we assume an isotropic distribution of radiation within the habitable volume thus simplifying the analysis. A framework for mission architectural optimization will be established here which will allow later specific designs to be introduced and optimized.

The habitable volume will be assumed to cover the entire solid angle with a constant thickness. The required crew living space will be for optimal performance and calculated assuming a right circular cylinder with 2.2 m height. The three critical organs (skin, lens, BFO) identified by the NCRP will be used in designing the shield as follows. Let R_j (x) be the dose equivalent rate to the j^{th} critical organ within a shield of thickness x calculated from the time dependent environments. We will ignore the several percent variations between 1 AU and 1.5 AU due to heliospheric diffusion. In addition to the GCR background, we will assume that if we are not within two years of solar minimum that a design limit solar event occurs (4 times Sept. 1989 event) and that an additional shelter is available which is a tolerable volume for such a short duration (see figure 1). We assume the shelter volume is a right circular cylinder of 2 m height with Tolerable living requirements. Dose rate and career dose limitations are required for the shield design process over the appropriate time intervals. For example, a mission to the L2 in three segments (Earth to L2 trip in time T_1, time on duty of T_2, and return trip of duration T_3) would first have to meet a requirement similar to

$$R_j(x_1)\,T_1 + R_j(x_2)\,T_2 + R_j\,(x_3)\,T_3 + H_{spe}(x_{spe}) < L_j \qquad (1)$$

where x_i is the shield thickness of the ith segment of the mission and L_j is the exposure limitation. The thirty day and annual dose rate constraints must be applied over each mission segment where the SPE drives the crew quarter shield design. We assume $x_1 = x_3$ for missions in which the transport vehicle is common to both transport segments with corresponding assumptions on required mass. The L_j is the accepted exposure limit to the j^{th} critical organ defined for LEO operations. Note, x_i, i = 1-3 are greater than 1 g/cm^2 in order to meet micrometeoroid impact requirements. Note, the above prescription does not account for the ALARA principle. Herein, the shelter is assigned to be the sleep quarters as one form of ALARA.

There are many combinations of x_1, x_2, x_3, and x_{spe} which satisfy the constraints above so that one must optimize the shielding by minimizing the total shield mass subject to the above constraints as follows:

$$\text{Min}\{V_s(x_1) + V_s(x_2) + V_s(x_3) + V_s(x_{spe})\} \cdot \rho = M_m \qquad (2)$$

where V_s is the shield volume of each mission segment associated with the required living volume of optimum performance or the crew quarter/shelter as appropriate. Note, $V_s(x_3)$ is set zero if the same transport vehicle is used in segments 1 and 3.

We now set up the logic for implementing the computational procedures outlined above. We will think beyond the optimization of a given vehicle or habitat and approach the problem of optimizing a given defined mission architecture. The first step in the process of finding an optimum mission architecture is specification of the mission start time, the sequence of mission segments with the associated required equipment, the crew member characteristics associated with each segment, the desired crew performance level on each segment, the construction materials for the shield on each segment, and the associated locations where the segment occurs. These aspects of the mission are described by elements of the mission architectural profile matrix as shown in table 5. Note that within this profile we only allow sequential mission segments and no multisegmented capability is allowed at this stage of development. Note, the last two row entries in table 5 will be taken as initial estimates of the design variables (shield thickness) to be optimized.

Table 5. Mission Architectural Profile Matrix

Mission title and start date: T_0				
Segment no.	1	2	3	…
Duration, days	T_1	T_2	T_3	…
Min. helio-radius	R_{min1}	R_{min2}	R_{min3}	…
Max. helio-radius	R_{max1}	R_{max2}	R_{max3}	…
Crew no.	N_1	N_2	N_3	…
Females	F_1	F_2	F_3	…
Min. age	FA_1	FA_2	FA_3	…
Males	M_1	M_2	M_3	…
Min. age	MA_1	MA_2	MA_3	…
Performance	$Perf_1$	$Perf_2$	$Perf_3$	…
Equipment	Eq_1	Eq_2	Eq_3	…
Location	Loc_1	Loc_2	Loc_3	…
Shield material	Mat_1	Mat_2	Mat_3	…
Shield thickness	x_1	x_2	x_3	…
Shelter thickness	δ_1	δ_2	δ_3	…

The mission duration is of course an important factor affecting the shield design. In addition, the crew size, composition, and expected performance levels all affect the shield design of the specific equipment required for a given segment. The total crew number and performance level (see figure 1 and table 3) will determine the volume of space required for a given segment and the associated wall area which must be shielded. The presence of females and their minimum age will often drive the dose rate constraints since the allowable career exposure of females is substantially less than males of the same age (see table 2). Age also determines the allowable career exposures for both males and females. Requiring the female crew to be approximately ten years older than their male counter parts effectively results in career limitations which no longer depend on gender.

In the present procedures, we will allow only a limited amount of hardware in the optimization process but will attempt to allow sufficient generality to expand to a more complex array of equipment, habitats, and vehicles. We will allow transfer vehicles for various transport segments of a mission allowing up to nine such unique vehicles denoted by indices of 1 through 9. If two segments use the same vehicle it will have the same index for each segment and a mapping of design thickness into a unique optimization parameter set must be made in the analysis. Similarly, each habitat will have a unique identifier denoted by index 11 to 19. This will constitute the only allowable hardware in the present study. Clearly this can be generalized by defining spacesuits as 21 to 29 and rovers as 31 to 39 and so on as required (see table 6)

Table 6. Mission equipment designation numbers.

Mission equip.	Designated indices, Eq_i
Transfer vehicles	1-9
Habitats	11-19
Spacesuits	21-29
Rovers	31-39
…	…

There are three locations where mission segments of interest may occur which are near earth for which we identify location indices as given in table 7. The deep space environment is represented as the GCR and SPE fluences measured at 1 AU and assumed to vary by less than 10 percent at distances currently accessible to human travel. Such a small variation for GCR has been observed and is described by various models. SPE may also vary little from here to Mars orbit since they result from the shock region at the front of a propagating coronal mass ejection (CME) and the propagating CME properties may vary little over propagation from 1 AU to 1.5 AU. The lunar and Martian environments are modified by interaction with surface materials and in addition for Mars the Martian atmosphere. These environments are applied as appropriately to the mission segments.

Table 7. Mission location indices

Location	Location index, Loc_i
Deep space	1
Lunar surface	2
Martian surface	3

The standard material associated with human activity has mainly been aluminum alloy 2219 although 6061 has also played a role. For construction of the walls of the habitable volume, other materials will generally provide greater protection. Many of these materials may be structural elements or materials on board for other purposes. The Graphite nanofiber/H is a hydrogenated herringbone graphite structure capable of absorbing

more than its weight of hydrogen. The current list of materials in the database and the associated material indices used in the present study are given in table 8. The last two entries into the mission profile are the shield wall thickness x_i and shelter/crew quarter thickness δ_i as initially estimated for each segment.

Table 8. Shield materials and material indices

Shield material	Materials index, Mat_i
Al 2219	1
Polyetherimide	2
Polysulfone	3
Polyethylene	4
Lithium hydride	5
Liquid methane	6
Graphite nanofiber/H	7
Liquid hydrogen	8

The first analysis task is to calculate the mission background dose rate to each critical organ over all the mission segments and configurations. This allows the assumption of a SPE at the worst time in each segment as will be treated subsequently. The background dose rates throughout the mission are established using the database on annual dose within the materials, the location, the specific equipment involved, and the specified shield thickness. The mission dose rate (per day) over the period t_{start} to $t_{start} + t_1 + t_2 + t_3 + \ldots$ is given as

$$R_j(t) = \begin{cases} H_{j1}(x_1, Eq_1, Mat_1, t)/365 & t_{start} \le t < t_{start} + t_1 \\ H_{j2}(x_2, Eq_2, Mat_2, t)/365 & t_{start}+t_1 \le t < t_{start}+t_1+t_2 \\ H_{j3}(x_3, Eq_3, Mat_3, t)/365 & t_{start}+t_1+t_2 \le t < t_{start} + .. \\ \ldots & \ldots \end{cases} \quad (3)$$

where appropriate equipment geometry and location is implied for each segment. Note, $R_j(t)$ is to be evaluated for each critical organ type j. The dose rate is used to establish exposure constraints and evaluation of the impact of a SPE on the mission design.

The dose rate for each segment depends on the time, the location, the equipment, and the shield material. Since the space radiation is isotropic one obtains some simplification in evaluating dose rate. The dose rate for the j^{th} critical organ and i^{th} segment within a transfer vehicle (e.g., Eq_i = 1 to 9) is given as

$$R_{ji}(x_i, Mat_i, t) = [0.6\, H_i(x_i, Mat_i, l=1, t) + 0.15\, H_j(30, Al, l=1, t) + 0.25\, H_j(60, Al, l=1, t)]/365 \quad (4)$$

where l = 1 denotes the location in Deep Space as is appropriate for the transfer and the contributions from Al accounts for the basic vehicle structure assumed to be constructed of Al 2219. The dose rate for a segment on the lunar or Mars surface will assume (for now) only exposures while in the habitat (e.g., Eq_i = 11 to 19) as

$$R_{ji}(x_i, Mat_i, t) = H_i(x_i, Mat_i, l=2 \text{ or } 3, t)/365 \quad (5)$$

where l = 2 or 3 denotes a location on the lunar or Martian surface. Of course, a habitat in space (say L2) would have l = 1. Effectively we assume only a small fraction of time is in an exploration EVA mode and adequate means of avoiding a SPE is available. These issues will be addressed in greater detail in a subsequent analysis. The associated shield mass depends on the number of crew N_i and the desired performance level $Perf_i$ as follows.

The habitable volume for a given performance level $Perf_i$ and duration t_i for either the transfer vehicle or habitat with N_i crew members is given by

$$V_i = V_{Perfi}(t_i)\, N_i \quad (6)$$

where the specific volume $V_{Perfi}(t_i)$ is given in figure 1 with $Perf_i$ the desired performance level and t_i the segment duration. Assuming a right circular cylinder of 2.2 m height, the associated cylindrical radius is

$$r_i = \sqrt{[V_i/(2.2\,\pi)]} \quad (7)$$

and the associated shield mass of the segment is

$$M_i(x_i) = \rho\pi\left(r_i + \frac{x_i}{100\rho}\right)^2\left(2.2 + \frac{x_i}{100\rho}\right) - 2.2\rho\pi r_i^2 \quad (8)$$

where x_i is the areal density of the shield material in g/cm^2 and ρ is the matter density (g/cm^3). The mass calculated by equation (8) is in metric ton. Multiply M_i's by 1000 to get the mass in kilogram units. In the present study we will assume that all equipment satisfies the same relations to performance level, crew size, and time.

The design must accommodate a possible SPE during any time except within two years of solar minimum. Furthermore, the exposure for any 30-day or annual period must satisfy dose rate constraints to prevent occurrence of deterministic effects. In this respect, we will allow for a very rare SPE which is 4x the September 29, 1989 event for design purposes and the assumption of an even larger event is on the order of few percent per year (only one such event seen in last 60 years). A storm shelter will be assumed to be the crew quarters where the crew spends a significant fraction of the day sleeping and in leisure activity and is placed within the habitable volume which is the primary shielded region. As such the shelter wall will be taken as $x_{spe} = x_i + \delta_i$ where δ_i represents the crew quarter wall shield thickness and assumed (for now) to be of the same material as the shield material for that segment. Similarly for SPE shelter is evaluated with Perf = 3 (Tolerable performance) for a duration of one day we have

$$V_{i,spe} = V_3(1\ d)\, N_i \quad (9)$$

Assuming the shelter to be a 2 m high right circular cylinder results in an associated cylindrical radius of

$$r_{i,spe} = \sqrt{[V_{i,spe}/(2\,\pi)]} \quad (10)$$

and the associated shelter shield mass is

$$M_{i,\,spe}(x_i) = \rho\,\pi\left(r_{l,spe} + \frac{\delta_i}{100\rho}\right)^2\left(2 + \frac{\delta_i}{100\rho}\right) - 2\rho\,\pi\, r^2_{l,\,spe} \quad (11)$$

We then run an accumulation assuming the SPE occurs in segment i as follows.

First we find the time of occurrence of the maximum of $H_i(x_i,t_{imax})$ as follows

$$\int_t^{t+\Delta} R_j(t')\,dt' + H_{j,spe}(x_{SPE})\,[1 - U(t,\Delta)] = H_j(t,\Delta) \qquad (12)$$

where $U(t,\Delta)$ is unity if both t or $t+\Delta$ are within two years of solar minimum and contains t_{imax}. We maximize $H_j(t,\Delta)$ for Δ = 1 month and 12 months on each segment i and each organ type j. We require

$$H_j(t_{max},\Delta) < L_j(\Delta) \qquad (13)$$

In addition to the dose rate constraints, the career limits constraint will be applied assuming no prior exposures as

$$\int R_j(t')\,dt' + H_{jspe}(x_{spe}) < L_j(age_{min},gender) \qquad (14)$$

assuming $H_{jspe}(x_{spe})$ as the maximum over all segments.

The mass of the shield that is to be minimized depends on the volume being protected and the areal density required to meet dose constraints. The specific volume (volume per crewmember) depends on duration and performance level as shown in figure 1. The total shield mass relation depends on the mission. For example, the Mars Reference Mission assumes that the transit to Mars and return to Earth are different vehicles so that the total mass is

$$M_n(x_1,x_2,x_3,\delta_1,\delta_2,\delta_3,) = M_1 + M_2 + M_3 + M_{1,spe} + M_{2,spe} + M_{3,spe} \qquad (15)$$

Whereas, the L2 mission (and lunar/asteroid missions) use ($M' = \max\{M_1,M_3\}$ and $x_1 = x_3$) so the total mass is

$$M_n(x_1,x_2,\delta_1,\delta_2) = M' + M_2 + M_{1,spe} + M_{2,spe} \qquad (16)$$

The corresponding mass is minimized over the unique equipment x_is and δ_is subject to constraints (13) and (14). In general, the mission mass is the sum over unique equipment used over all the segments

$$M = \Sigma M_i \qquad (17)$$

The computational procedure must account for all of these specific mission aspects. We now define the baseline reference missions for which the trades will be evaluated.

REFERENCE MISSION ARCHITECTURE PROFILES

In this section, we will define the Reference missions against which trades will be made. The missions to be considered are the near Earth 100 day class missions such as a lunar or L2 mission and the more distant 1000 day class missions such as Mars or asteroid exploration. The craft reference construction material will always be taken as Aluminum 2219 alloy. This is the dominant material used in the Shuttle and International Space Station and represents current standard practice. The initial mission profile matrix will be given along with the optimized results to be used as a baseline for further study.

L2 REFERENCE MISSION -There are several possible missions to L2 for not only space science but as a possible gateway to deep space exploration to asteroids or Mars. A reference profile for the L2 mission is for 18 days in transit from and back to LEO with a 26-day mission stay. The crew size is taken as four members with careers in midlife. The optimized profile for aluminum 2219 is shown in table 9.

Table 9. L2 Reference Mission Architectural Profile Matrix

$L2/T_0$ = 1/1/2014			
Segment no.	1	2	3
Duration, days	18	26	18
Min. helio-radius, AU	1.0	1.0	1.0
Max. helio-radius, AU	1.0	1.0	1.0
Crew no.	4	4	4
Females	2	2	2
Min. age	40	40	40
Males	2	2	2
Min. age	40	40	40
Performance	1	1	1
Equipment	1	1	1
Location	1	1	1
Shield material	1	1	1
Shield thickness, g/cm^2	1	1	1
Shelter thickness, g/cm^2	34.76	34.768	34.76

Table 10. Lunar Reference Mission Architectural Profile Matrix

Lunar/T_0 = 3/6/2018							
Segment no.	1	2	3	4	5	6	7
Duration, days	4.5	2	2	30	2	2	4.5
Min. helio-radius, AU	1.	1.	1.	1.	1.	1.	1.
Max. helio-radius, AU	1.	1.	1.	1.	1.	1.	1.
Crew no.	4	4	4	4	4	4	4
Females	2	2	2	2	2	2	2
Min. age	40	40	40	40	40	40	40
Males	2	2	2	2	2	2	2
Min. age	40	40	40	40	40	40	40
Performance	1	1	1	1	1	1	1
Equipment	1	11	2	12	2	11	1
Location	1	1	1	2	1	1	1
Shield material index	1	1	1	1	1	1	1
Shield thickness, g/cm^2	1	1	1	1	1	1	1
Shelter thickness, g/cm^2	1	1	1	1	1	1	1

.

LUNAR REFERENCE MISSION-The lunar reference mission will be taken as a 4.5-day transit to an L1 with a 2-day layover followed by a 2-day trip to the lunar

surface. The surface stay is for 30 days followed by a 2-day return to L1 with a second 2-day layover followed by a 4.5-day return to LEO. The crew size is taken as four middle aged men and women of equal numbers. The optimized reference profile is given in table 10. This mission falls within two years of Solar minimum and no SPE is expected to occur. Minimum shielding is required and material type plays no role.

MARS REFERENCE MISSION-The Mars reference mission is described elsewhere [11] and consists of 180 - day Mars transit to Mars orbit with descent to the surface for a 500-day exploration segment and a 180-day return in a separate vehicle. The initial estimates of dose equivalent to the three critical organs during the Mars reference mission were evaluated using the above described methods, the dose equivalent rate to the lens and BFO are shown in figures 9 and 10. The dose equivalent rate to the BFO for the profile matrix in Table 11 is shown in figure 11. The maximum of the integral of the background over thirty day intervals about each time in the mission given in equation (13) as

$$H(\Delta) = \int_t^{t+\Delta} R_j(t')\, dt' \qquad (18)$$

is shown in figure 12 for the BFO. The time of maximum background exposure over the time period of 30 days is shown in the figure and are the times of the assumed solar particle event if outside of the two years from solar minimum where significant solar events are observed to occur. These times of SPE occurrence are shown in figure 12 and are the times used in equation (13) in the design process. Similar results are also derived for the annual exposure limitations. The integral over the entire mission as

$$H_{GCR} = \int R_j(t')\, dt' \qquad (19)$$

is likewise evaluated for estimation of the career limit exposures as appearing in equation (14). These evaluations provide the constraints for the beginning iteration of the optimization procedure.

The baseline Mars Reference Mission profile is given in table 11. It is not practical to optimize for this mission with Al shielding material since exposure limitations require the aluminum shield to be in excess of 100 g/cm^2. These values of shield and shelter thickness are the maximum allowable values allowed in the optimization procedure.

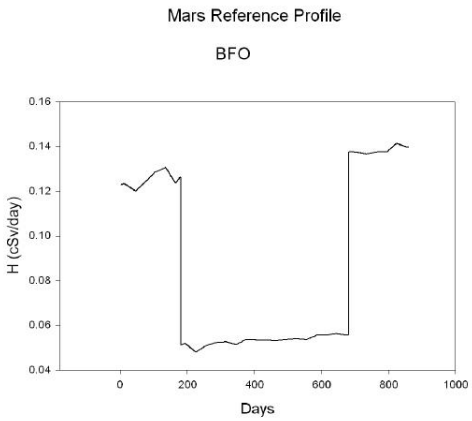

Fig. 11. BFO background dose equivalent rate during the Mars reference mission for the table 11 profile matrix.

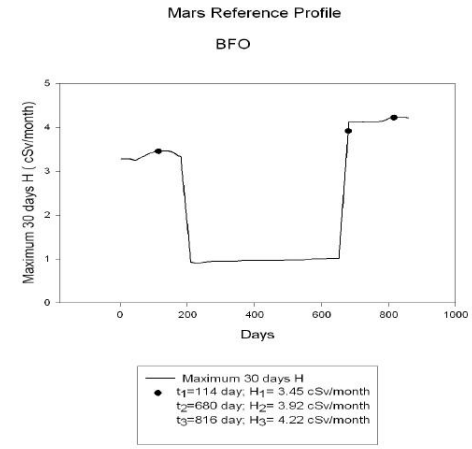

Fig. 12. Thirty day BFO background dose equivalent during the Mars reference mission for the table 11 profile matrix.

Table 11. Mars Reference Mission Architectural Profile Matrix

Mars Ref. Mission: T_0 = 2014			
Segment no.	1	2	3
Duration, days	180	500	180
Min. helio-radius, AU	1.0	1.5	1.0
Max. helio-radius, AU	1.5	1.5	1.5
Crew no.	6	6	6
Females	2	2	2
Min. age	40	41	42
Males	4	4	4
Min. age	40	41	42
Performance	1	1	1
Equipment	1	11	1
Location	1	3	1
Shield material	1	1	1
Shield thickness, g/cm^2	100	100	100
Shelter thickness, g/cm^2	100	100	100

MARS/VENUS SWINGBYREFERENCE MISSION- A second Mars reference mission has a Venus swingby consisting of 104 day transfer with helio-radius minimum of 0.722 AU. After Mars orbit is achieved, the crew spends 5 days in orbit before descent to the surface for a 30-day stay. Launch to Mars orbit with a second 5-day stay before returning to Earth during a 221-day transit. This reference mission architecture profile is given in table 12. Note, we have used the lunar surface environment as an approximation to Mars orbit. This will account for the Martian shadow but the neutron component is slightly overestimated. It is not practical to optimize for this mission with Al shielding material. And the values of shield and shelter thickness are the maximum values allowed in the optimization procedure.

Table 12. Mars/Venus Swingby Reference Mission Architectural Profile Matrix

Mars Ref. Mission: T_0 = June 3, 2018					
Segment no.	1	2	3	4	5
Duration, days	104	5	30	5	221
Min. helio-radius, AU	0.72	1.5	1.5	1.5	1.0
Max. helio-radius, AU	1.5	1.5	1.5	1.5	1.5
Crew no.	6	6	6	6	6
Females	2	2	2	2	2
Min. age at start	40	40	40	40	40
Males	4	4	4	4	4
Min. age at start	40	40	40	40	40
Performance	1	1	1	1	1
Equipment	1	1	11	1	1
Location	1	2*	3	2*	1
Shield material	1	1	1	1	1
Shield thickness, g/cm^2	100	100	100	100	100
Shelter thickness, g/cm^2	100	100	100	100	100

* used to approximate Mars orbit

SHIELD MATERIALS TRADE STUDIES

In this section, we will define and discuss the material trades made for the reference missions described in the earlier section.

L2 MISSION MATERIAL TRADES – Trades have been studied for the L2 reference mission given in table 9 for the materials of table 4. The optimized mass for using various materials is shown in figure 13. As an example an optimized profile for graphite nanofibers is shown in table 13 and the associated shield mass is found to be 2 ton and is achieved using the graphite nanofiber/H experimental energy storage material.

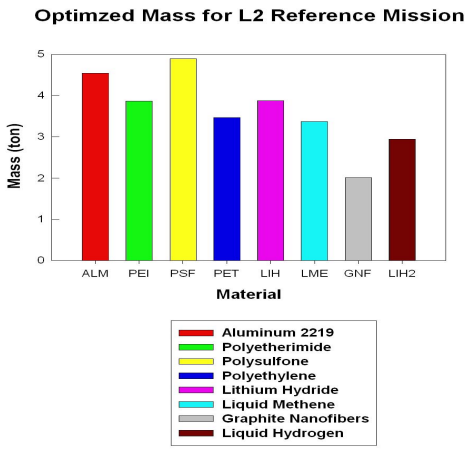

Fig. 13. Optimized mass for L2 reference and trade missions for various materials.

Table 13. L2 Mission Material Trade Architectural Profile Matrix

L2/ T_0 = 1/1/2014			
Segment no.	1	2	3
Duration, days	18	26	18
Min. helio-radius, AU	1.0	1.0	1.0
Max. helio-radius, AU	1.0	1.0	1.0
Crew no.	4	4	4
Females	2	2	2
Min. age	40	40	40
Males	2	2	2
Min. age	40	40	40
Performance	1	1	1
Equipment	1	1	1
Location	1	1	1
Shield material	7	7	7
Shield thickness, g/cm^2	1	1	1
Shelter thickness, g/cm^2	14.	14	14

LUNAR MISSION MATERIAL TRADES-The lunar mission material trade has been studied for the reference mission profile given in table 10 and the optimized mass is shown in figure 14. This mission falls within two years of Solar minimum and no SPE is expected to occur. Minimum shielding is required and material type plays no essential role. As a result table 10 is also the profile for trades for all the materials.

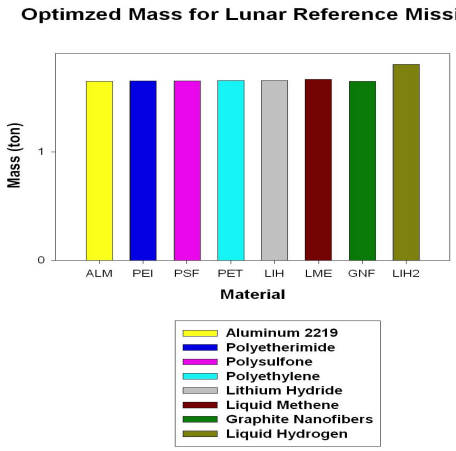

Fig. 14. Optimized mass for Lunar reference and trade missions for various materials.

MARS REFERENCE MISSION MATERIAL TRADES- It is interesting to note that there is no optimum solution for the mass within the constraints imposed in the present study for the baseline Mars Reference Mission profile given in table 11. The trade studies were done for all the materials of table 4. Figure 15 shows the mass of the materials where optimization could be achieved. An optimized trade profile is given in table 14 and the associated shield mass is found to be 182.6 t.

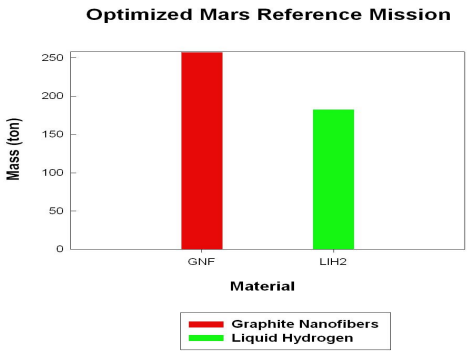

Fig. 15. Optimized mass for Mars trade missions for various materials.

Table 14. Optimized Mars Mission Material Trade Architectural Profile Matrix

Mars Ref. Mission: T_0 = 2014			
Segment no.	1	2	3
Duration, days	180	500	180
Min. helio-radius, AU	1.0	1.5	1.0
Max. helio-radius, AU	1.5	1.5	1.5
Crew no.	6	6	6
Females	2	2	2
Min. age	40	41	42
Males	4	4	4
Min. age	40	41	42
Performance	1	1	1
Equipment	1	11	2
Location	1	3	1
Shield material	8	8	8
Shield thickness, g/cm^2	27	29.4	30
Shelter thickness, g/cm^2	23	1	11.2

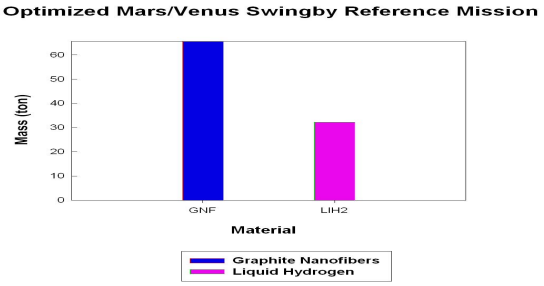

Fig. 16. Optimized mass for Mars/Venus Swingby Trade missions for two materials. See text for details.

Table 15. Mars/Venus Swingby Mission Material Trade Architectural Profile Matrix

Mars Ref. Mission: T_0 = June 3, 2018					
Segment no.	1	2	3	4	5
Duration, days	104	5	30	5	221
Min. helio-radius, AU	0.72	1.5	1.5	1.5	1.0
Max. helio-radius, AU	1.5	1.5	1.5	1.5	1.5
Crew no.	6	6	6	6	6
Females	2	2	2	2	2
Min. age at start	40	40	40	40	40
Males	4	4	4	4	4
Min. age at start	40	40	40	40	40
Performance	1	1	1	1	1
Equipment	1	1	11	1	1
Location	1	2*	3	2*	1
Shield material	8	8	8	8	8
Shield thickness, g/cm^2	16.5	16.5	1	16.5	16.5
Shelter thickness, g/cm^2	1	1	1	1	1

- used to approximate Mars orbit

MARS/VENUS SWINGBY MISSION TRADES- In the study of the second Mars reference mission architecture profile of table 12 optimization was not practical with Al shielding material. Figure 16 gives the optimized mass of the materials where it could be achieved. And table 15 gives the optimized profile for liquid hydrogen trade for the mission. The associated optimized mass is 32.2 t.

CREW AGE TRADE STUDIES

There is a sensitivity of optimization on age. As an example, for the Mars profile of table 16, optimization has been studied for all materials listed in table 4 with varying age of 55 and below until optimization is possible. For a given material type, im, at each age, ia, the shield and shelter thickness are varied between 1 and 100 g/cm^2 till an optimized profile that satisfies the constraints is found. Figure 17 shows the optimized mass with age for the heaviest (Al 2219) and the lightest (liquid hydrogen) materials. Optimization is not practical when shield and shelter thickness between 1 and 100 g/cm^2 cannot be found that satisfies the constraints. For Al 2219 the minimum age for optimized profile is 50 years. Figure 18 shows the optimized mass for different materials at age 50. The shield and shelter thickness shown in table 16 are the initial starting thickness. There is an interesting feature to the optimization process in finding the optimum thickness. At higher ages, e.g. at 55, shield thickness is 1 g/cm^2 and the optimization is achieved by varying the shelter thickness. As the age is lowered progressively shield thickness increases and the shelter thickness decreases till at certain age optimization is not possible. The minimum age down to which optimization is possible depends on the material considered (see Fig. 17). Figure 18 gives the optimized mass and Figure 19 shows the figure of merit of different materials at 55 years.

Table 16. Mars/Venus Swingby Trade Mission Architectural Profile Matrix

Mars Ref. Mission: T_0 = January 10, 2009/2031					
Segment no.	1	2	3	4	5
Duration, days	313	5	30	5	302
Min. helio-radius, AU	0.72	1.5	1.5	1.5	1.0
Max. helio-radius, AU	1.5	1.5	1.5	1.5	1.5
Crew no.	6	6	6	6	6
Females	2	2	2	2	2
Min. age at start	ia	ia	ia	ia	ia
Males	4	4	4	4	4
Min. age at start	ia	ia	ia	ia	ia
Performance	1	1	1	1	1
Equipment	1	1	11	1	1
Location	1	2*	3	2*	1
Shield material	im	im	im	im	im
Shield thickness, g/cm^2	1	1	1	1	1
Shelter thickness, g/cm^2	1	1	1	1	1

* used to approximate Mars orbit

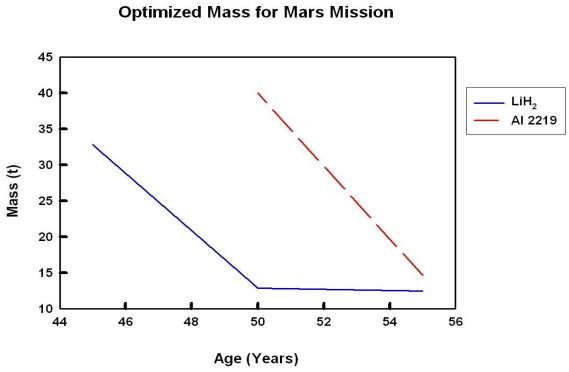

Fig. 17. Optimized mass for mars mission for the profile given in Table 16 for Al 2219 and Liquid Hydrogen (LiH2) representing two extremes of the materials considered in the report.

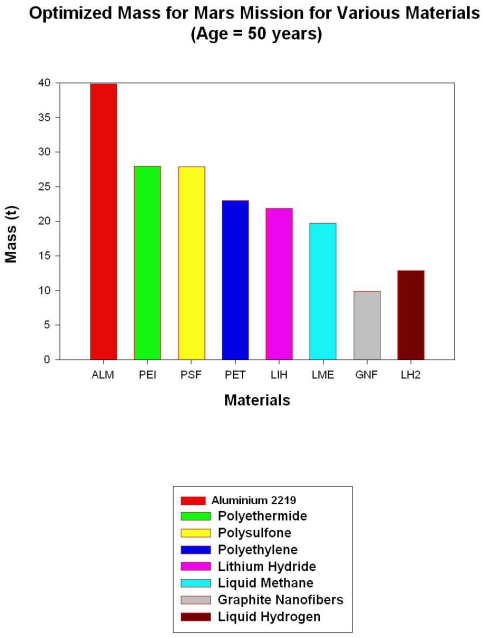

Fig. 18. Optimized mass for mars mission for the profile given in Table 16 for various materials for age 50 (the minimum age of optimization for Al 2219).

Note that the optimized solution depends on the chemical composition and the material density since a very light material like LH2 occupies a large volume leaving the more compact mass of the graphite nanofiber/H as the minimum mass material because of its higher density.

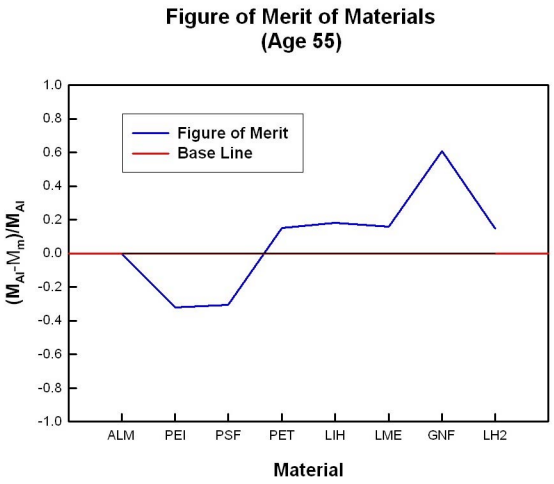

Fig. 19. Figure of merit for various materials for 55 years for Mars profile matrix table 16.

CONCLUSION

The method provides an optimization procedure for radiation shielding for deep space missions. The total shield mass over all pieces of equipment and habitats is optimized over multi-segmented missions involving multiple work and living areas subject to career dose and dose rate constraints. Studies have been made for L2, Lunar, Mars and Mars/Venus swing-by reference missions. For all these missions, material trades have been studied. And, as an example, a crew age trade for Mars/Venus swing-by mission has been done. The career blood forming organ (BFO) constraints are more stringent and play a critical role in the optimization procedure. The short missions to L2 and the Moon mainly need to deal with the possibility of solar particle events. It is found that improved shield materials will be required to enable a Mars mission in which middle-aged astronauts can participate. If the age of the astronauts are allowed to be 55 and older then more options are available. Only a sample of trades has been accomplished in the present paper which mainly concerned setting up the computational procedures. Added analysis functionality will be added to the process at a latter date. The procedure provides a welcome tool for optimized radiation shield design.

REFERENCES

1. Wilson, J.W. et al. Chapter 1: Preliminary considerations. *Shielding Strategies for Human Space Exploration.* NASA CP 3360, 1997.
2. Wilson, J.W. et al, Issues in deep space radiation protection. *Astronautica Acta.* In press.
3. National Council on Radiation Protection &Measurements, *Guidance on Radiation Received in Space.* NCRP Report 98, 1989.
4. National Council on Radiation Protection &Measurements, *Radiation Protection Guidance for Activities in Low Earth Orbit.* NCRP Report 132, 2001.
5. Woolford, B. et al. Chapter 12: Human factors implications for shielding. *Shielding Strategies for Human Space Exploration.* NASA CP 3360, 1997.
6. Badhwar, G.D. and O'Neill, P.M., Improved model of galactic cosmic radiation for space exploration mission, Nucl. Tracks & Radiat., 20, 403-410, 1992
7. Badhwar G.D., et. al, Intercomparison of radiation measurements on STS-63;, Radiat. Meas. 26; 147-158; 1997
8. Wilson, J.W., Kim M-H, Shinn, J.L., Tai, H., Cucinotta, F.A., Badhwar, G.D., Badavi, F.F., Atwell, W.: Solar Cycle Variation and Application to the Space Radiation Environment, NASA/TP-1999-209369
9. Kim, M-H., Wilson, J.W., Simonsen, L.C., Cucinotta, F.A., Atwell, W., Badavi, F.F., Miller, J.: Contribution of High Charge and Energy (HZE) Ions During Solar-Particle Event of September 29, 1989, NASA/TP-19999-209320.
10. Clowdsley, M. S. et al., Can. J. Phys. 78: 45-56; 2000.
11. Hoffman, S.J. and Kaplan, D.I.; Human Exploration of Mars: The Reference Mission of the NASA Mars Exploration Study Team, NASA Special Publication 6107

CONTACT

The communicating author email address is:
r.k.tripathi@larc.nasa.gov